

HIGH-FREQUENCY MONITORING OF GROWTH-AT-RISK

LAURENT FERRARA, MATTEO MOGLIANI, AND JEAN-GUILLAUME SAHUC

ABSTRACT. Monitoring changes in financial conditions provides valuable information on the contribution of financial risks to future economic growth. For that purpose, central banks need real-time indicators to promptly adjust their policy stance. In this paper, we extend the quarterly Growth-at-Risk (GaR) approach of [Adrian et al. \(2019\)](#) by accounting for the high-frequency nature of financial conditions indicators. Specifically, we use Bayesian mixed data sampling (MIDAS) quantile regressions to exploit the information content of both a financial stress index and a financial conditions index leading to real-time high-frequency GaR measures for the euro area. We show that our daily GaR indicator (i) displays good GDP nowcasting properties and (ii) can provide an early signal of GDP downturns. During the first six months of the Covid-19 pandemic period, it has provided a timely measure of tail risks weighing on the euro area GDP.

JEL: C22, E37, E44.

Keywords: Growth-at-Risk, mixed-data sampling, Bayesian quantile regressions, financial conditions, euro area.

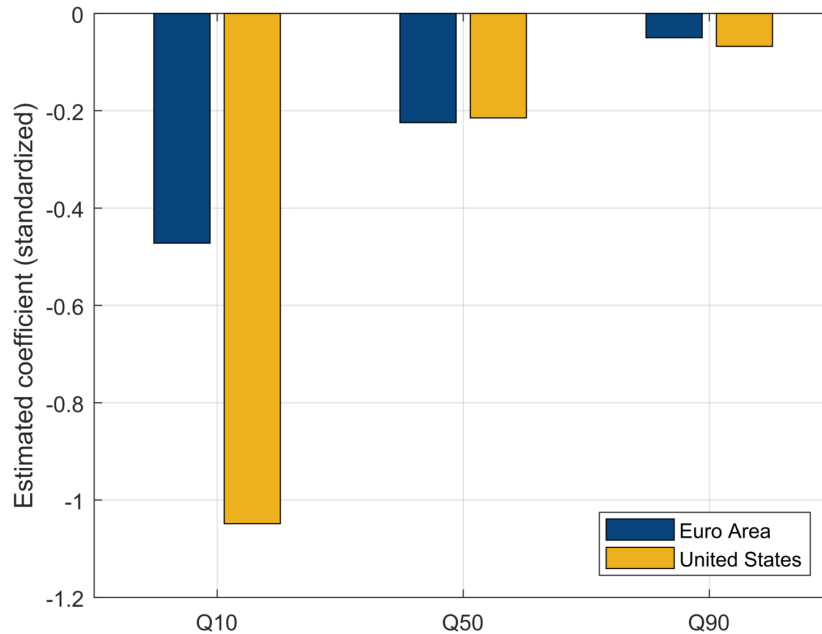
1. INTRODUCTION

There is a growing body of research, from both theoretical and empirical literature, suggesting that the information content of financial indicators is relevant for macroeconomic forecasting and that financial shocks are influential in driving global activity.¹ It follows that a good understanding of the evolution of economic conditions would require to monitor the tension in the financial sector. Based on this observation, [Adrian et al. \(2019\)](#) developed a tool for evaluating financial risks to economic growth, using a tail-risk approach known as the Growth-at-Risk (GaR), that can be seen as equivalent to the Value-at-Risk concept in finance. This approach is used to keep track of the distortion of the entire expected growth distribution according to financial market developments using quantile regression methods ([Giglio et al., 2016](#)). Quantile regressions provide an estimate of the elasticity of

April 2021. L. Ferrara: SKEMA Business School, France (e-mail: laurent.ferrara@skema.edu). M. Mogliani: Banque de France, 31 rue Croix des Petits Champs, 75049 Paris, France (e-mail: matteo.mogliani@banque-france.fr). J.-G. Sahuc: Banque de France, 31 rue Croix des Petits Champs, 75049 Paris, France (e-mail: jean-guillaume.sahuc@banque-france.fr). We would like to thank Pierre Pinson (Editor), two anonymous referees, the participants of the 2019 Conference on Real-Time Data Analysis, Methods and Applications, 2020 International Institute of Forecasters Virtual Workshop (Economic Forecasting in Times of Covid-19), Virtual International Symposium of Forecasting 2020, OFCE seminar, Essex Business School seminar and 2nd European Commission workshop on *Big data and economic forecasting* for their useful comments and suggestions. The views expressed in this paper are those of the authors and do not necessarily reflect the views of the Banque de France or the Eurosystem. Declarations of interest: none.

¹A few prominent contributions are [Nolan and Thoenissen \(2009\)](#), [Helbling et al. \(2011\)](#), [Claessens et al. \(2012\)](#), [Jermann and Quadrini \(2012\)](#), [Gilchrist and Zakrajsek \(2012\)](#), [Christiano et al. \(2014\)](#), [Lopez-Salido et al. \(2017\)](#).

FIGURE 1. Elasticity of GDP growth to quarterly financial conditions for different quantiles



Notes: Q10, Q50 and Q90 represent the 10% quantile, 50% quantile (or median) and 90% quantile, respectively. Estimates are obtained by replicating the one-step ahead quarterly model in [Adrian et al. \(2019\)](#) over the 2001q1-2019q4 sample. The euro-area financial conditions index is the one proposed by [Petronovich and Sahuc \(2019\)](#) and the U.S. financial conditions index comes from the Chicago Fed (NFCI).

the Gross Domestic Product (GDP) growth rate to financial conditions for any range of values of the economic growth rate, thus capturing the non-linear nature of this relationship. Figure 1 displays the values of these elasticities for various quantiles in the United States and the euro area and shows that the relationship is strongest for changes in GDP located at the bottom of the distribution. This illustrates that a tightening of financial conditions tends to amplify the effects of negative shocks to the real economy, as notably emphasized by [Bernanke and Gertler \(1989\)](#), while an easing of these conditions has a more limited impact on economic activity at the peak of the cycle.

However, the standard GaR approach suffers from several drawbacks arising primarily from a modelling of tail-risks based on quarterly data, while financial indicators are often sampled at higher frequency. To ensure the same frequency, financial conditions indexes are usually aggregated by simple averaging to get the data sampled at the same low-frequency as GDP. Such data aggregation is likely to lead to biased estimates if the underlying data generating process does not feature a flat-aggregation scheme from high to low frequencies. Asymptotically inefficient and inconsistent estimates may hence dampen the information content of daily financial indicators and have adverse effects on forecasting. In addition, this strategy makes the standard GaR relying on somewhat outdated financial information, the latter usually entering the model with one quarter lag, while central banks need the most current information to adjust promptly their policy stance. Higher-frequency data series are thus

helpful to more accurately assess economic conditions, as evidenced by [Clements and Galvao \(2009\)](#), [Rodriguez and Puggioni \(2010\)](#), [Schorfheide and Song \(2015\)](#), [Ghysels \(2016\)](#), [Mazzi and Mitchell \(2020\)](#), [Lima et al. \(2020\)](#) or [Carriero et al. \(2020\)](#). More particularly, [Andreou et al. \(2013\)](#) show that model regressions exploiting high-frequency financial data series provide a substantial gain as regards current and next quarter output growth forecasting accuracy, against various benchmark models as well as survey forecasts.

In this paper, we implement a mixed data sampling (MIDAS) quantile regression approach ([Ghysels et al., 2016](#)) to obtain a real-time high-frequency GaR measure. More specifically, we consider a bayesian approach for estimation ([Korobilis, 2017](#); [Carriero et al., 2020](#)) and a restricted Almon lag polynomial approximation of the high-frequency component ([Mogliani and Simoni, 2021](#)).² We then consider the 10th percent quantile of the conditional predictive distribution of current euro area GDP growth – which is akin to nowcasting – and compute a high-frequency measure of current tail-risks on activity that we call the *daily* GaR(10%). Our model combines the information stemming from two daily euro area financial indicators in order to better capture different features of the financial side of the economy: (i) the Composite Indicator of Systemic Stress (CISS) of the European Central Bank ([Holló et al., 2012](#)) and (ii) the financial indicator proposed by [Petronевич and Sahuc \(2019\)](#). The first one is a financial stress indicator, which is designed to react more to systemic fragility in financial markets, whereas the second one is a financial conditions index, which is more useful in exploring macro-financial linkages. We also collect seasonally and calendar adjusted vintages of quarterly GDP into a real-time triangle spanning from 1999Q1 to 2020Q2 to perform an historical analysis on a pseudo real-time basis.

We propose several applications to highlight the practical interest of our daily GaR(10%) measure. We first evaluate the nowcasting ability of our model, *i.e.* the ability to assess current GDP growth, based on the entire predictive distribution. Second, we look at the real-time evolution of the indicator before and during a specific recession episode, namely the sovereign debt crisis that affected the euro area from 2010 to 2013. Third, we inspect the link between the GaR measure and the main unconventional monetary policy decisions announced by the ECB between 2013 and 2018. Finally, we focus on the Covid-19 pandemic period during the first half-2020, which offers an interesting case study for assessing extreme macroeconomic risks through our high-frequency measure.

We show that our high-frequency approach provides an efficient monitoring of financial risks weighing on the euro area. For instance, our daily GaR(10%) measure would have led to an advanced detection of the GDP downturn observed during the European sovereign debt crisis, by steadily declining by approximately 1 percentage point, more than a quarter ahead of the start of the recession in 2011Q4.

²[Carriero et al. \(2020\)](#) show that Bayesian mixed frequency quantile regressions may provide superior predictive accuracy compared to the frequentist approach.

In addition, it provides a day-to-day benchmark for monetary policy by revealing information about how economic activity is likely to react to new announcements. We observe in particular an increase in the value of the GaR(10%) around (either following or anticipating, consistently with the narrative and the expectations prevailing at that time) each announcement of the main unconventional monetary policies between 2013 and 2018. Finally, during the first half-2020, it has provided a timely indication of tail risks on euro-area GDP, especially since the World Health Organization (WHO) announcement recognizing the Covid-19 epidemic as a global pandemic on March 11th, 2020.

Our paper contributes to the very recent literature on the use of quantile regressions to evaluate macroeconomic risks (see [Giglio et al., 2016](#), [Adrian et al., 2019](#), [Gonzalez-Rivera et al., 2019](#), or [Figueres and Jarocinski, 2020](#), [Adams et al., forthcoming](#)), as well as on mixed frequency data models to assess current economic conditions. In addition, we do not solely focus on nowcasting but also propose a new piece to the policymakers' toolkit for real-time macro-financial surveillance.

In the remainder of the paper, Section 2 introduces the Growth-at-Risk approach with mixed data sampling and describes the bayesian approach. Section 3 presents the data and the computational approach. Section 4 proposes some applications, including a focus on the Covid-19 crisis, and Section 5 concludes.

2. GROWTH-AT-RISK WITH MIXED FREQUENCY DATA SAMPLING

2.1. The Growth-at-Risk approach. Since the Global Financial Crisis and the ensuing Great Recession in 2008-09, financial institutions have step up their monitoring of financial conditions in order to be able to rapidly react to any possible financial shocks before its transmission to the real economy. [Adrian et al. \(2019\)](#) have recently developed a methodology, referred to as Growth-at-Risk (GaR), for measuring financial risks or vulnerabilities to U.S. economic growth. This approach is now widely used by the International Monetary Fund to assess risks to the global financial system in its flagship biannual *Global Financial Stability Report* (see, for instance, [IMF, 2019](#)).

The GaR approach relies on a quantile regression of GDP growth on past financial conditions and past GDP, accounting thus for non-linearities in a very simple econometric model of macro-financial linkages. Indeed, both theoretical and empirical literature have shown that financial markets play a key role in the transmission and propagation of shocks to the economy, but the channels of transmission are highly complex and present a strong degree of non-linearity. For instance, building on earlier theoretical contributions such as [Bernanke and Gertler \(1989\)](#), [Carlstrom and Fuerst \(1997\)](#), [Kiyotaki and Moore \(1997\)](#) or [Bernanke et al. \(1999\)](#), the recent literature shows that financial constraints can lead to highly nonlinear dynamics in the economy's response to shocks (asymmetric impulse responses following a negative or a positive shock). Recently, [Hubrich and Tetlow \(2015\)](#) have empirically assessed models of financial frictions and have shown that (i) a single-regime model of

the macroeconomy and financial stress is inadequate to capture the dynamics of the economy and (ii) output reacts more strongly to financial shocks in times of financial stress than in normal times.

As in [Adrian et al. \(2019\)](#), let us assume that we want to assess the joint effect of past GDP growth (y_{t-h}) and a given financial conditions indicator (x_{t-h}), where h is the forecast horizon, on the current GDP growth (y_t). Furthermore, consider an additional vector \mathbf{w}_{t-h} of K control variables. We assume at this stage that both the target variable and the vector of regressors have been sampled at the same quarterly frequency. The methodology dealing with frequency mismatches is the core of this paper and will be presented in the following section. Beyond the standard linear ordinary least squares (OLS) approach, the quantile regression framework put forward by [Koenker and Bassett \(1978\)](#) is an efficient way to introduce non-linearities in the relationship between a given variable y_t and its predictors. Instead of minimizing the sum of squared errors, as in the OLS approach, the quantile estimation is based on the asymmetric minimization of the weighted absolute errors.

Let's consider the following quantile regression:

$$y_t = \beta_1(\tau)y_{t-h} + \beta_2(\tau)x_{t-h} + \gamma(\tau)' \mathbf{w}_{t-h} + \epsilon_t, \quad (1)$$

where the vector of coefficients $\boldsymbol{\beta}(\tau) := (\beta_1(\tau), \beta_2(\tau), \gamma(\tau)')'$ depends on the τ -th quantile of the random error term ϵ_t . The coefficients $\hat{\boldsymbol{\beta}}(\tau)$ are obtained by minimizing the following loss function:

$$\sum_{t=1}^T \rho_\tau(y_t - \boldsymbol{\beta}(\tau)' \mathbf{z}_{t-h}), \quad (2)$$

where $\mathbf{z}_{t-h} = (y_{t-h}, x_{t-h}, \mathbf{w}_{t-h})'$, $\rho_\tau(u) = u(\tau - I(u < 0))$ is the check loss function, with $I(\cdot)$ denoting the indicator function. [Koenker and Bassett \(1978\)](#) proved that the predicted value $\hat{Q}_{y_t}(\tau|\mathbf{z}) = \hat{\boldsymbol{\beta}}(\tau)' \mathbf{z}_{t-h}$ is a consistent linear estimator of the conditional quantile function of y_t . In order to provide an evaluation of financial risks to future economic activity, an estimate of the future quantile function of $y_{T|T-h}$, conditional on sample information available up to $T - h$, is given by:

$$\hat{Q}_{y_{T|T-h}}(\tau|\mathbf{z}) = \hat{\boldsymbol{\beta}}(\tau)' \mathbf{z}_{T-h}. \quad (3)$$

Based on estimates of the conditional quantile function over a discrete number of quantile levels, it is possible to estimate the full continuous conditional distribution of $y_{T|T-h}$. As in [Adrian et al. \(2019\)](#), we choose to fit a flexible distribution, known as the generalized Skewed-Student distribution, in order to smooth the estimated conditional quantile function of $y_{T|T-h}$ and recover a probability density function.³ This specific distribution allows for fat tails and asymmetry and boils down to the Normal distribution as a specific case. The generalized Skewed-Student distribution has the following

³As noted by [Adrian et al. \(2019\)](#), Equation (3) represents an approximate estimate of the quantile function, which is difficult to map into a probability distribution function due to approximation error and estimation noise.

density function:

$$f(y; \mu, \sigma, \alpha, \nu) = \frac{2}{\sigma} t\left(\frac{y - \mu}{\sigma}; \nu\right) T\left(\alpha \frac{y - \mu}{\sigma} \sqrt{\frac{\nu + 1}{\nu + \left(\frac{y - \mu}{\sigma}\right)^2}}; \nu + 1\right), \quad (4)$$

where μ is a location parameter, σ a scale parameter, ν a fatness parameter and α a shape parameter. $t(\cdot)$ and $T(\cdot)$ are respectively the probability density function (*pdf*) and the cumulative density function (*cdf*) of the standard Student distribution (Azzalini and Capitanio, 2003).

In practice, the four parameters of the generalized Skewed-Student distribution are estimated through a quantile matching approach aiming at minimizing the squared distance between the estimated conditional quantile functions and the inverse *cdf* of the generalized Skewed-Student distribution given by:

$$\min_{\mu, \sigma, \alpha, \nu} \sum_{\tau} \left[\widehat{Q}_{y_{T|T-h}}(\tau | \mathbf{z}) - F^{-1}(\tau; \mu, \sigma, \alpha, \nu) \right]^2, \quad (5)$$

where $F^{-1}(\cdot)$ is the inverse cumulative Skewed-Student distribution. Finally, from the fitted quantile function, $F^{-1}(\tau; \widehat{\mu}, \widehat{\sigma}, \widehat{\alpha}, \widehat{\nu})$, it is possible to compute some downside risk measures, such as the expected shortfall, at any given probability level. Due to the short data sample used in our empirical part, we shall focus on the lower 10th percent quantile of the predicted distribution (see also Figueres and Jarocinski, 2020), called the GaR(10%), which is given by:

$$Q_{y_{T|T-h}}^*(\tau = 0.10 | \mathbf{z}) := F^{-1}(\tau = 0.10; \widehat{\mu}, \widehat{\sigma}, \widehat{\alpha}, \widehat{\nu}). \quad (6)$$

This can be interpreted as the expected value of future GDP at 10% probability, stemming from the conditional quantile function of $y_{T|T-h}$.

2.2. Introducing the MIDAS-quantile regression. The problem with the setup described above is that both the aggregation of high-frequency (financial) indicators into the lower frequency of GDP and the lag structure of the specification in Equation (1), prevent the model from reacting readily to sudden shocks. Hence, from the policymaker point of view, the GaR model appears an impractical tool for monitoring financial risks to activity in real-time.

We thus propose to adapt Equation (1) to account for the possible high-frequency nature of the regressors. Let us assume that the financial indicator x_t is available on a daily basis, *i.e.* virtually without delay, and denote it $x_t^{(d)}$ (*i.e.* it is observed about $d = 60$ times on average between quarters $t - 1$ and t). Further, let us note that also the set of control variables can be sampled at higher frequency than the target variable. Hence, for notation convenience and consistently with the applications presented in the next sections, let us assume that $K = 1$ and that w_t is sampled at monthly frequency, and let us denote it $w_t^{(m)}$, with $m = 3$. According to these features, we can build a high-frequency real-time

GaR measure which relates current quarterly GDP growth to past *and* current values (up to the latest available observation) of high-frequency financial conditions and the control variable. For this purpose, the general model used throughout this paper follows a mixed data sampling (MIDAS)-quantile regression (MIDAS-QR):

$$y_t = \beta_1(\tau)y_{t-1} + \beta_2(\tau) \sum_{c=0}^{C_x-1} \tilde{B}(c; \theta_x(\tau)) L^{c/d} x_{t-h_d}^{(d)} + \gamma(\tau) \sum_{c=0}^{C_w-1} \tilde{B}(c; \theta_w(\tau)) L^{c/m} w_{t-h_m}^{(m)} + \epsilon_t \quad (7)$$

where $\tilde{B}(c; \theta_j(\tau))$ is a weighting function (normalized to sum up to 1), which depends on a vector of parameters $\theta_j(\tau)$, for $j = \{x, w\}$, and a lag order c . Note that the forecast horizon is expressed in high-frequency terms ($h_f = 0, 1/f, 2/f, \dots, (C_j - 1)/f$, for $f = \{d, m\}$). While [Ghysels et al. \(2016\)](#) propose the Beta lag polynomial function for the quantile weighting function, we choose a simple polynomial approximation of the underlying true weighting structure provided by the (un-normalized) Almon lag polynomial $B(c; \theta_j(\tau)) = \sum_{i=0}^p \theta_{i,j}(\tau) c^i$, where $\theta_j(\tau) := (\theta_{0,j}(\tau), \theta_{1,j}(\tau), \dots, \theta_{p,j}(\tau))'$, similarly to [Lima et al. \(2020\)](#) and [Mogliani and Simoni \(2021\)](#). Under the so-called "direct method", Equation (7) with (un-normalized) Almon lag polynomials can be reparameterized as:

$$y_t = \beta_1(\tau)y_{t-1} + \theta_x(\tau)' \tilde{\mathbf{x}}_{t-h_d}^{(d)} + \theta_w(\tau)' \tilde{\mathbf{w}}_{t-h_m}^{(m)} + \epsilon_t, \quad (8)$$

where $\theta_x(\tau)$ and $\theta_w(\tau)$ are vectors featuring $(p+1)$ parameters, $\tilde{\mathbf{x}}_t^{(d)} := \mathbf{Q}_x \mathbf{x}_t^{(d)}$ and $\tilde{\mathbf{w}}_t^{(m)} := \mathbf{Q}_w \mathbf{w}_t^{(m)}$ are $((p+1) \times 1)$ vectors of linear combinations of the observed high-frequency variables, $\mathbf{x}_t^{(d)} := (x_t^{(d)}, x_{t-1/d}^{(d)}, \dots, x_{t-(C_x-1)/d}^{(d)})'$ and $\mathbf{w}_t^{(m)} := (w_t^{(m)}, w_{t-1/m}^{(m)}, \dots, w_{t-(C_w-1)/m}^{(m)})'$ are $(C_j \times 1)$ vectors of high-frequency lags, and \mathbf{Q}_j is a $(p+1 \times C_j)$ polynomial weighting matrix (for $j = \{x, w\}$), with $(i+1)$ -th row $[0^i, 1^i, 2^i, \dots, (C_j-1)^i]$ for $i = 0, \dots, p$. Note that estimates of the slope coefficients $\beta_2(\tau)$ and $\gamma(\tau)$ in Equation (7) can be computed as $\hat{\beta}_2(\tau) = \hat{\theta}_x(\tau)' \mathbf{Q}_x \iota_{C_x}$ and $\hat{\gamma}(\tau) = \hat{\theta}_w(\tau)' \mathbf{Q}_w \iota_{C_w}$, where ι_{C_j} is a $(C_j \times 1)$ vector of ones.

The main advantage of the Almon lag polynomial is that Equation (8) is linear and parsimonious, as it depends only on $(p+1)$ parameters for the high-frequency variable. Further, linear restrictions on the value and slope of the lag polynomial $B(c; \theta_j(\tau))$ may be placed for any $c \in (0, C_j - 1)$. Endpoint restrictions, such as $B(C_j - 1; \theta_j(\tau)) = 0$ and $\nabla_c B(c; \theta_j(\tau))|_{c=C_j-1} = 0$, may be desirable and economically meaningful, as they jointly constrain the weighting structure to tail off slowly to zero ([Mogliani and Simoni, 2021](#)). As a result, the number of parameters in Equation (8) reduces from $(p+1)$ to $(p-r+1)$, where $r \leq p$ is the number of restrictions.

2.3. Bayesian estimation. In the standard quantile regression ([Koenker and Bassett, 1978](#)), the distribution of the residuals ϵ_t in Equation (8) is unspecified (a non-parametric distribution) and the estimation of the τ -th quantile regression coefficients is the solution to the minimization of the loss

function given by (2). Let's denote $\mathbf{X}_t = (y_{t-1}, \tilde{\mathbf{x}}_{t-h_d}^{(d)}, \tilde{\mathbf{w}}_{T-h_m}^{(m)})'$ and $\Theta(\tau) = (\beta_1(\tau), \boldsymbol{\theta}_x(\tau)', \boldsymbol{\theta}_w(\tau)')$. Yu and Moyeed (2001) showed that the minimization of $\sum_{t=1}^T \rho_\tau(y_t - \Theta(\tau)' \mathbf{X}_t)$ is equivalent to maximizing a likelihood function under the asymmetric Laplace error distribution (ALD) for ϵ_t .⁴ According to Kozumi and Kobayashi (2011), the ALD $f(\epsilon|\sigma)$ can be viewed as a mixture of an exponential and a scaled Normal distribution. Considering the random variables $\nu \sim \text{Exp}(1)$ and $\omega \sim \mathcal{N}(0, 1)$, then $\epsilon = \xi_1 \sigma \nu + \xi_2 \sigma \sqrt{\nu} \omega$ follows the skewed distribution $f(\epsilon|\sigma)$ above, with:

$$\xi_1 = \frac{1-2\tau}{\tau(1-\tau)} \quad \text{and} \quad \xi_2^2 = \frac{2}{\tau(1-\tau)}.$$

Hence, using this expression for ϵ , we can rewrite Equation (8) as:

$$y_t = \Theta(\tau)' \mathbf{X}_t + \xi_1 \tilde{\nu}_t + \xi_2 \sqrt{\sigma \tilde{\nu}_t} \omega_t, \quad (9)$$

where $\tilde{\nu}_t = \sigma \nu_t$ follows the exponential distribution $\text{Exp}(\sigma)$, with density function $f(\tilde{\nu}_t|\sigma) = \sigma^{-1} \exp(-\tilde{\nu}_t/\sigma)$. Then, the conditional likelihood function stems from a Normal distribution and takes the following form:

$$f(y|\mathbf{X}, \Theta, \tilde{\nu}, \sigma, \tau) \propto \prod_{t=1}^T \frac{1}{\xi_2 \sqrt{\sigma \tilde{\nu}_t}} \exp \left[-\frac{1}{2} \sum_{t=1}^T \frac{(y_t - \Theta(\tau)' \mathbf{X}_t - \xi_1 \tilde{\nu}_t)^2}{\xi_2^2 \sigma \tilde{\nu}_t} \right].$$

We consider standard conditionally Normal prior that leads to the following hierarchical representation of the Bayesian MIDAS quantile regression (BMIDAS-QR):

$$y|\mathbf{X}, \Theta, \sigma, \tilde{\nu}, \tau \sim \mathcal{N}(\Theta(\tau)' \mathbf{X}_t + \xi_1 \tilde{\nu}_t, \xi_2^2 \sigma \tilde{\nu}),$$

$$\Theta|\tau \sim \mathcal{N}(\Theta_0, \Sigma_0),$$

$$\tilde{\nu}|\sigma \sim \text{Exp}(\sigma),$$

$$\sigma \sim \text{Inv-Gamma}(a_1, b_1).$$

As shown notably by Khare and Hobert (2012), the full conditional posteriors are given by:

$$\Theta|\mathbf{X}, \sigma, \tilde{\nu}, \tau \sim \mathcal{N}(\mathbf{A}^{-1} \mathbf{B}, \mathbf{A}^{-1}),$$

$$\tilde{\nu}_t|\mathbf{X}, \Theta, \sigma, \tau \sim \text{GiG} \left(\frac{1}{2}, \frac{(y_t - \Theta(\tau)' \mathbf{X}_t)}{\xi_2^2 \sigma \tilde{\nu}_t}, \frac{\xi_1^2 + 2\xi_2^2}{\sigma \xi_2^2} \tilde{\nu}_t \right),$$

⁴The ALD has density

$$f(\epsilon|\sigma) = \frac{\tau(1-\tau)}{\sigma} \exp \left[-\frac{\rho_\tau(\epsilon)}{\sigma} \right],$$

and moments:

$$E(\epsilon) = \sigma \frac{1-2\tau}{\tau(1-\tau)} \quad V(\epsilon) = \sigma^2 \frac{1-2\tau(1-\tau)}{\tau^2(1-\tau)^2}.$$

Both theoretical and empirical results support the use of the ALD in the context of quantile regressions, even when the true distribution of the data is not ALD (Sriram et al., 2013).

$$\sigma | \mathbf{X}, \Theta, \tilde{v}, \tau \sim \text{inv-Gamma} \left(\frac{3T}{2} + a_1, \sum_{t=1}^T \frac{(y_t - \Theta(\tau)' \mathbf{X}_t - \zeta_1 \tilde{v}_t)^2}{2\zeta_2^2 \tilde{v}_t} + \sum_{t=1}^T \tilde{v}_t + b_1 \right),$$

where $\mathbf{A} = (\mathbf{X}'_t \mathbf{D}^{-1} \mathbf{X}_t + \Sigma_0^{-1})^{-1}$, $\mathbf{B} = \mathbf{X}'_t \mathbf{D}^{-1} (y_t - \zeta_1 \tilde{v}) + \Sigma_0^{-1} \Theta_0$, and $\mathbf{D} = \text{diag}(\zeta_2^2 \sigma \tilde{v}_t)$.

3. DATA AND COMPUTATIONAL APPROACH

3.1. Data. In our applications, we focus on recent events that have impacted the euro area economy. As an aggregate measure of economic activity, we use the quarter-on-quarter growth rate of GDP for the euro area as whole (Figure 2a). To perform the analysis on a pseudo real-time basis, we collect seasonally and calendar adjusted vintages of quarterly GDP from Eurostat and ECB. The data are composed of multiple releases for the same vintage (preliminary flash estimates, flash estimates and regular estimates), whose number and publication delays vary overtime, and are collected into a real-time triangle spanning from 1999Q1 to 2019Q4. Actual historical release dates are also identified and matched with each vintage.

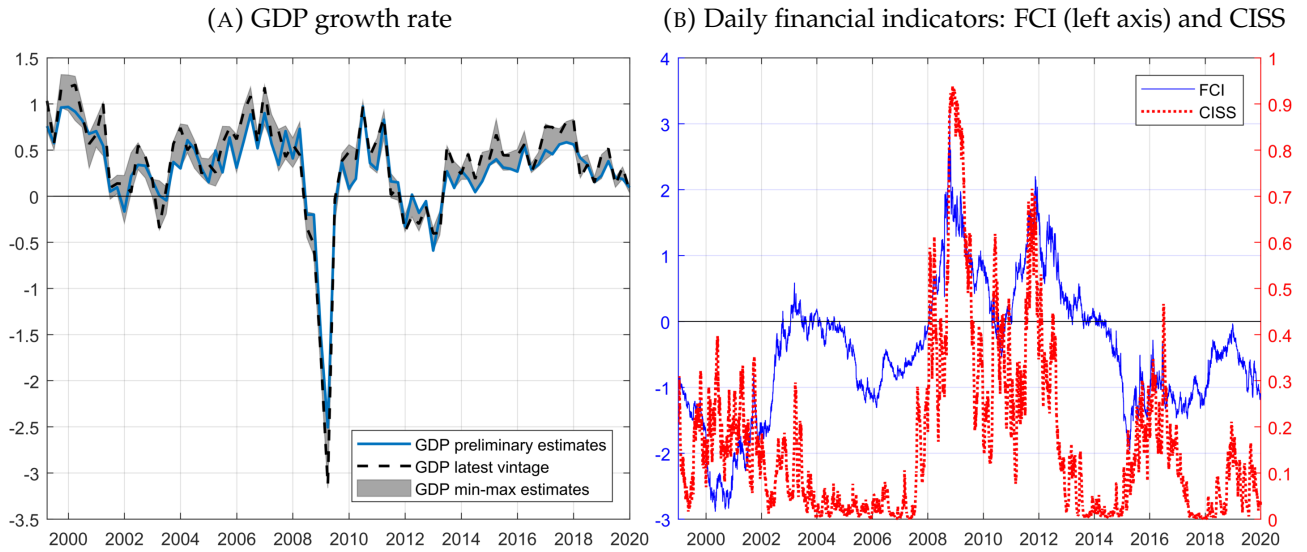
As regards the high-frequency financial indicators, we consider two alternative daily euro area time series: (i) a financial stress indicator, which is designed to react to systemic fragilities within financial markets, and (ii) a financial conditions index, which is more useful in exploring macro-financial linkages. The two indicators complement each other in capturing different features of the financial side of the economy, as can be seen on Figure 2b.⁵

The financial stress indicator is the Composite Indicator of Systemic Stress (CISS) developed by the European Central Bank (Holló et al., 2012). The main methodological innovation of the CISS is the application of basic portfolio theory to the aggregation of five market-specific sub-indexes, namely the foreign exchange market, the equity market, the money market, the bond market and the financial intermediaries. The aggregation takes into account time-varying cross-correlations between the five sub-indexes. As a result, the CISS puts relatively more weight on situations in which stress prevails in several market segments at the same time, capturing the idea that financial stress is more systemic and thus more dangerous for the economy as a whole if financial instability spreads more widely across the whole financial system. Holló et al. (2012) proposed the determination of critical levels for the CISS using the endogenous outcomes of two econometric regime-switching models.

The financial conditions index (FCI) is the one proposed by Petronevich and Sahuc (2019). This new FCI is based on six main components (rates, credit, equity, uncertainty, inflation, and exchange rates) extracted from eighteen daily series through a principal component analysis. The FCI is then

⁵Both financial indicators are freely available on the European Central Bank Statistical Data Warehouse (CISS) and on the Banque de France Webstat (FCI), respectively.

FIGURE 2. Euro area GDP and daily financial conditions indices (1999-2019)



Notes: Panel A displays the GDP growth rate with the uncertainty associated with the estimates represented by the gray area. Panel B plots the two euro-area daily financial indicators: the financial conditions index (FCI) proposed by [Petronевич and Sahuc \(2019\)](#) and the composite indicator of systemic stress (CISS) proposed by [Holló et al. \(2012\)](#).

computed by aggregating these components using time-varying weights, which are based on univariate conditional volatilities estimated through a GARCH(1,1) model. As greater volatility increases the weight of the corresponding component, the FCI may put relatively more weight on single stressed components, whose signal is hence not muted by the state of the other components. As a result, the FCI resorts on information stemming from the actual level of the components and their volatility.

Finally, we control for macroeconomic news by setting $w_t^{(m)}$ as the Euro area Composite Purchasing Managers Index Output (PMI hereafter).⁶ This choice is dictated by the fact that the financial indicators considered are not explicitly designed to reflect real side developments and expectations, although they may indirectly capture such signals. Controlling for real factors can be important to gauge the real-time effect of financial indicators on real activity (see also [Plagborg-Møller et al., 2020](#) and [De Santis and Van der Veken, 2020](#)). In this sense, survey data, such as PMI, provide timely and mostly unrevised macroeconomic news information that can be easily exploited in our mixed-frequency framework.

3.2. Computing the high-frequency GaR(10%). As shown in Figure 2b, the FCI and the CISS present very similar high-frequency patterns, pointing to a strong correlation between these two series. Using the two indicators together in quantile regression (10) would then likely introduce multicollinearity in the model, leading to poor inference and predictive results. Hence, the first step for the construction of our GaR(10%) measure consists in estimating regression (9) through the Bayesian approach described

⁶We thank an anonymous referee for this suggestion.

in Section 2.3 and using two distinct set of regressors \mathbf{X} . Both include one lag of GDP growth and the PMI, but only one financial indicator, *i.e.* either the FCI or the CISS. In the regressions we use a third-degree Almon lag polynomial ($p = 3$) and two end-point restrictions ($r = 2$) for both daily and monthly predictors, and we set the high-frequency lag windows to $C_x = 60$ (days) and $C_w = 6$ (months). We use standard diffuse priors for the model parameters Θ and σ , except for the autoregressive lag of GDP, whose prior mean and variance are set such that the probability mass is concentrated below unity. The Gibbs sampler is run for $N = 250,000$ iterations, with the first 50,000 used as burn-in period, and every 10th draw is saved. The estimation sample spans 1999Q1 to 2019Q4 and the daily forecasts start on July 1st, 2009.

Let's denote $\widehat{Q}_{i,y_{T|T-h_d}}^{(n)}(\tau|\mathbf{X}_i)$ the n -th posterior conditional quantile estimate of $y_{T|T-h_d}$ provided by the Markov Chain Monte Carlo (MCMC) algorithm, for $n = 1, \dots, N$. The subscript i denotes whether the underlying specification includes the FCI ($i = 1$) or the CISS ($i = 2$). The τ -th conditional quantile point estimate is then given by:

$$\widehat{Q}_{i,y_{T|T-h_d}}(\tau|\mathbf{X}_i) = \frac{1}{N} \sum_{n=1}^N \widehat{Q}_{i,y_{T|T-h_d}}^{(n)}(\tau|\mathbf{X}_i),$$

that is the average predicted value from regression (9) for each quantile τ .⁷ The generalized Skewed-Student distribution is then fitted on $\widehat{Q}_{i,y_{T|T-h_d}}(\tau|\mathbf{X}_i)$, and we hence recover our **high-frequency daily GaR(10%)** indicator (see Equation (6)):

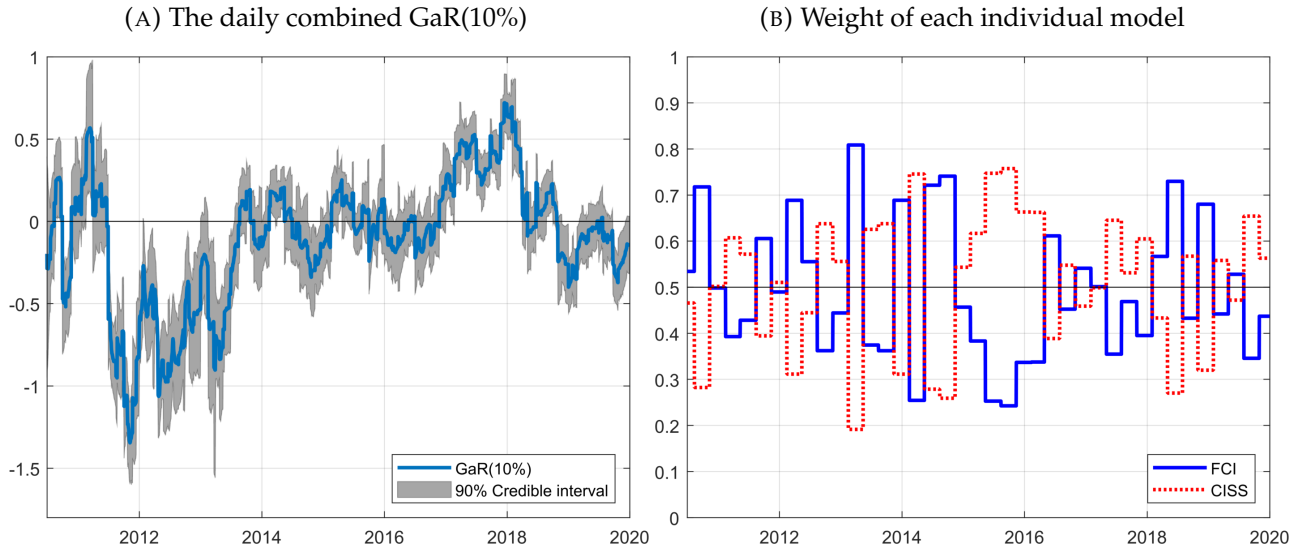
$$Q_{i,y_{T|T-h_d}}^*(\tau = 0.10|\mathbf{X}_i). \quad (10)$$

Finally, note that the Bayesian estimation provides a natural estimate of the standard error of the quantile function, as the conditional likelihood implies that the conditional quantile function is normally distributed. We can hence provide a measure of uncertainty surrounding the estimated daily GaR(10%) by computing its credible interval at some $(1 - \alpha)$ level. In order to obtain asymptotically valid credible intervals, we implement the correction to the covariance matrix of the posterior chain proposed by [Yang et al. \(2016\)](#).

3.3. Combining Growth-at-Risk measures. In the previous step, we computed competing Gar(10%) measures, based on two alternative –although broadly complementary– financial indicators. However, for the ease of analysis and interpretation of the results, it would be preferable from the policy-maker point of view to summarize the information stemming from these two indicators into a single GaR measure. For this purpose, we adopt a strategy based on density forecasts combination (see for

⁷It is worth noting that y_{T-1} is not available until its actual publication, usually around 30-45 days after the end of quarter $T - 1$. To overcome this issue without affecting the real-time nature of the analysis, we use the EuroCoin indicator as a proxy of past GDP growth. This indicator is released by the end of quarter $T - 1$, and real-time vintages are available on the [CEPR](#) website.

FIGURE 3. The daily combined GaR(10%) and the weight associated with each individual model, over the 2010Q3–2019Q4 period



Note: The daily combined GaR(10%) corresponds to the lower 10th percentile of the distribution of the expected real GDP growth, based on the combination of two individual GaR(10%) measures, estimated from models including each a different financial conditions indicator (FCI or CISS).

instance [Hall and Mitchell, 2007](#), and [Geweke and Amisano, 2011](#)). More specifically, we implement the following algorithm:

- (1) From Section 3.2, the individual smoothed conditional predictive quantile functions $Q_{i,y_{T|T-h_d}}^*(\tau|\mathbf{X}_i)$, for $\tau \in (0, 1)$, are computed sequentially (*i.e.* on a daily basis from July 1st, 2009 onwards) for each specification including either the FCI ($i = 1$) or the CISS ($i = 2$).
- (2) The individual predictive quantile functions are then converted into density forecasts and a real-time measure of their predictive performance is computed. We choose the Quantile Weighted Probability Score (QWPS; [Gneiting and Ranjan, 2011](#)), which provides a metrics for the evaluation of the predictive ability of a model by emphasising the (left) tail of the estimated density forecasts.⁸
- (3) Combination weights $\omega_{i,T-h_d}$ are computed recursively (*i.e.* from the first to the last business day of each quarter) using a discounted QWPS combinations method, similar to the point

⁸The QWPS is a quantile-weighted version of the CRPS ([Gneiting and Raftery, 2007](#)), given by $\text{QWPS}(f, y) = \int_0^1 \text{QS}_\tau(F^{-1}(\tau), y) \nu(\tau) d\tau$, where $\text{QS}_\tau(F^{-1}(\tau), y)$ is the quantile score and $\nu(\tau)$ is a weighting function. While $\nu(\tau) = 1$ leads to the standard CRPS, in our application we chose $\nu(\tau) = (1 - \tau)^2$, which emphasise the left tail of the predictive distribution and reflects implicitly an asymmetric loss function weighing more on lower quantiles. Alternative popular metrics for combining density forecasts, such as the log-Score or the CRPS (see [Geweke and Amisano, 2011](#), and [Pettenuzzo et al., 2016](#), among others) provided nevertheless very similar results.

forecast approach of [Stock and Watson \(2004\)](#) and [Andreou et al. \(2013\)](#):

$$\omega_{i,T-h_d} = \frac{w_{i,T-h_d}^{-\kappa}}{\sum_i w_{i,T-h_d}^{-\kappa}},$$

where

$$w_{i,T-h_d} = \sum_{j=T_0}^{T_\ell} \delta^{T_\ell-j} \text{QWPS}_{i,j},$$

with $\kappa = 2$, $\delta = 0.9$ (the discount factor), T_0 the point at which the first prediction is computed, and T_ℓ the point at which the most recent prediction can be evaluated in real-time.⁹

(4) Finally, the combined conditional predictive quantile function is computed recursively as:

$$Q_{y_{T|T-h_d}}^*(\tau|\mathbf{X}) = \sum_i \omega_{i,T-h_d} \times Q_{i,y_{T|T-h_d}}^*(\tau|\mathbf{X}_i).$$

From the obtained combined quantile function, we recover the high-frequency (daily) *combined* GaR(10%) indicator $Q_{y_{T|T-h_d}}^*(\tau = 0.10|\mathbf{X})$. This daily indicator, along with its estimated 90% credible interval, as well as the evolution of the weights $\omega_{i,T-h_d}$, are presented in [Figure 3](#) (panel A and B, respectively) over the period 2010Q3-2019Q4.¹⁰

4. EMPIRICAL RESULTS

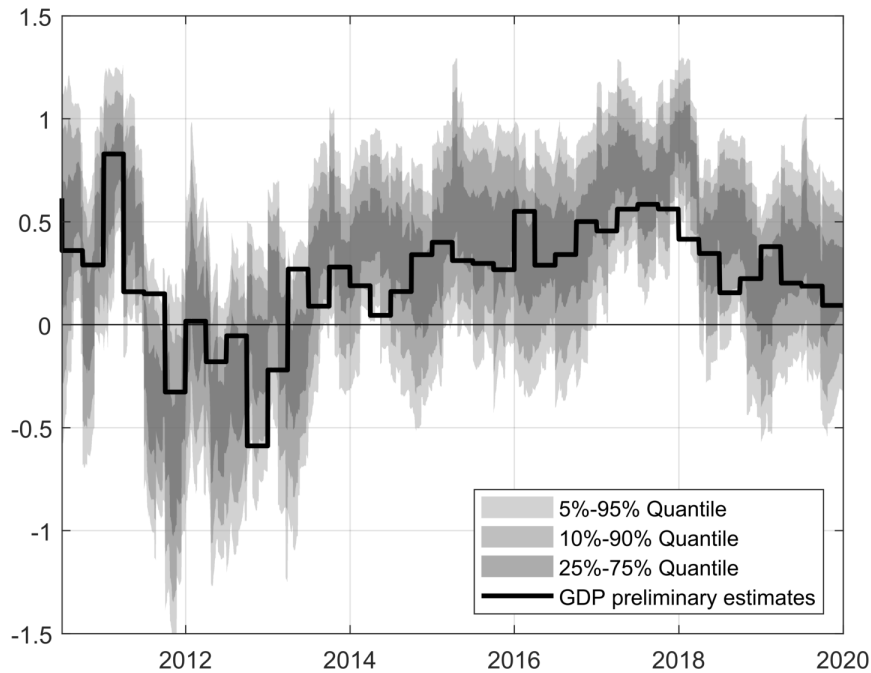
This section presents four applications on the euro area economy which illustrate the practical interest of using a daily GaR measure. In the first application, we evaluate its nowcasting properties when trying to track in real-time GDP growth. A second application focuses on the real-time evolution of the indicator during the European sovereign debt crisis. The third one highlights its strong link with the main monetary policy decisions taken between 2013 and 2018. Finally, we evaluate the behaviour of our high-frequency measure during the first six months of the Covid-19 pandemic.

4.1. Nowcasting GDP. As a first illustration, we evaluate the overall nowcasting performance of our BMIDAS-QR model, beyond the GaR measure. For this purpose, we consider the predictive densities obtained from the conditional predictive quantile function $Q_{y_{T|T-h_d}}^*(\tau|\mathbf{X})$. These densities are reported

⁹Given the size of the evaluation sample, we do not compute specific weights for each forecast horizon h_d , but we stack $\text{QWPS}_{i,T-h_d}$ in a single vector. Further, because of the pseudo real-time nature of the analysis, $T_\ell \neq T - h_d$. It follows that $\omega_{i,T-h_d} = \omega_{i,T-(h_d+1)}$ as long as a new point is available for evaluation. Finally, we use the first 97 daily predictions, from July 1st, 2009 to June 30th, 2010, to warm-up the combination scheme. Over the period July 1st, 2009 - November 12th, 2009, we initialise the combination weights by setting $\omega_{i,T-h_d} = 0.5$.

¹⁰The daily GaR(10%) series is obtained overtime in a pseudo real-time manner: every daily prediction corresponds to a specific h_d forecast horizon, depending on the date of the prediction and the number of business days in the quarter. For instance, the GaR(10%) value for June 30 corresponds to the prediction obtained from a specification with $h_d = 0$, while the value for April 30 corresponds to the prediction obtained from a specification with $h_d = 40$ (on average).

FIGURE 4. Nowcasting GDP with the BMIDAS-QR model



Note: The BMIDAS-QR model is the Bayesian mixed data sampling (MIDAS) model linking quarterly GDP and daily financial conditions indices estimated with quantile regression (QR) methodology.

in Figure 4, along with the preliminary estimates of quarterly GDP. A visual inspection of the figure suggests that the conditional distributions can track the actual GDP growth fairly well, notably during the 2011-2013 recession episode (see Section 4.2), as well as during the acceleration of activity in 2016-2017 and the following deceleration in 2018-2019.

Forecasts from our model are first compared to those from a benchmark specification, given by a simple Bayesian AR(1) regression (BAR). Consistently with the conditional distribution approach investigated in the present paper, we concentrate mainly on density forecasts, which are evaluated by the means of four various criteria: average log-Score differentials (LS), average Continuous Ranking Probability Score ratios (CRPS; [Gneiting and Raftery, 2007](#)), average Quantile-Weighted Probability Score ratios (QWPS; [Gneiting and Ranjan, 2011](#)) and average Quantile Score ratios (QS). For CRPS, QWPS and QS criteria, values less than one indicate that our combined model outperforms the benchmark. For the LS criterion, positive values indicate that our model produces more accurate density forecasts than the BAR. As a robustness check, we further consider density forecasts from two competing models, namely a combined Bayesian MIDAS model (BMIDAS) and a Bayesian Quantile AR(1) regression (BQAR). Combined BMIDAS density forecasts are computed using the same combination strategy as outlined in Section 3.3, where the underlying univariate models and densities are estimated

TABLE 1. Out-of-sample results: relative accuracy of density forecasts (2010Q3-2019Q4)

h_d	BMIDAS-QR				BMIDAS				BQAR(1)			
	LS	CRPS	QWPS	QS(0.10)	LS	CRPS	QWPS	QS(0.10)	LS	CRPS	QWPS	QS(0.10)
0	0.30	0.81	0.81	0.64	0.23	0.90	0.83	0.63	0.11	0.97	0.98	0.98
10	0.22	0.91	0.86	0.60	0.19	0.95	0.85	0.61	0.11	0.97	0.98	0.98
20	0.26	0.88	0.84	0.60	0.20	0.94	0.85	0.62	0.11	0.97	0.98	0.97
40	0.09	1.05	1.10	0.88	0.03	1.13	1.10	0.84	0.07	0.99	1.01	0.92
60	0.11	1.03	1.08	0.87	0.02	1.10	1.08	0.82	0.08	0.99	1.00	0.92

Notes: LS, CRPS, QWPS, and QS denote respectively the log-score, the continuously ranked probability score, the quantile weighted probability score, and the quantile score (evaluated at $\tau = 0.10$), in relative terms with respect to the BAR(1) benchmark. Bold values denote the best outcomes across the models considered for each forecast horizon h_d .

using the approach described in [Pettenuzzo et al. \(2016\)](#). The BQAR model is similar to specification (8) but with only the lagged GDP in the quantile regression.

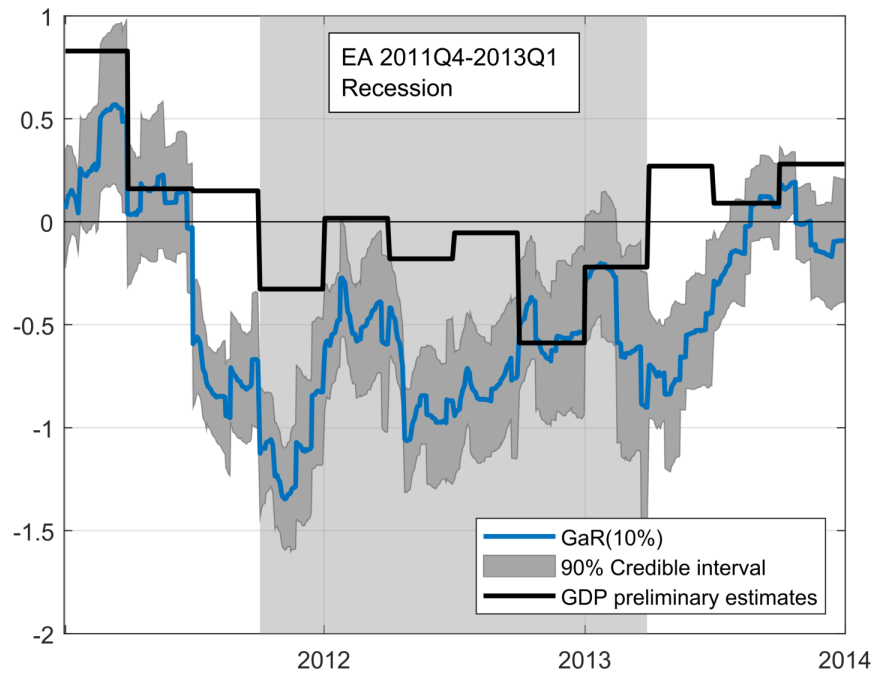
The results, reported in Table 1, point to a systematic outperformance of our BMIDAS-QR model with respect to the BAR(1) benchmark and the other competitors considered for relatively short forecast horizons (up to 20 business days). For longer horizons, this evidence is less clear-cut, as our model appears to outperform the competitors only according to the log-score criterion, while the results mostly favour the BQAR(1) regression. It is nevertheless worth noting that our model tends to outperform, although sometimes only slightly, the combined BMIDAS regressions, which embed exactly the same information as our quantile regressions.¹¹

All in all, the empirical evidence reported here supports the importance of accounting for nonlinearities when modelling and predicting real activity with financial indicators. Moreover, our results appear consistent with those for the United States reported by [Plagborg-Møller et al. \(2020\)](#), suggesting that financial data can provide accurate and timely indications of downward risks to GDP growth in the short-term, while their contribution fades away as macroeconomic information becomes progressively available.

4.2. The European sovereign debt crisis. As a second illustration, we take the example of the European sovereign debt crisis that affected the euro area from 2010 to 2013. The 2008 financial crisis had indeed left its mark on public finances, leading to a significant increase in government bond yield spreads. Despite a rescue package for Greece, financial tensions intensified again due to the worsening of public finances in several other euro area countries and to the contagion arising from the undertaken agreement to restructuring the Greek sovereign debt by mid-July 2011. The sovereign

¹¹According to the tests proposed by [Rossi and Sekhposyan \(2019\)](#), we can reject the null hypothesis of correct calibration of the predictive densities of the BMIDAS-QR model at a 5% level only. In addition, the Diebold-Mariano-West test ([Diebold and Mariano, 1995](#); [West, 1996](#)) for unconditional equal predictive accuracy (computed over point and density forecasts) tends to statistically support the outperformance of the BMIDAS-QR model over the BMIDAS model.

FIGURE 5. The GaR(10%) during the euro- area sovereign debt crisis



Note: The GaR(10%) corresponds to the lower 10th percentile of the distribution of the expected real GDP growth.

debt crisis increasingly turned into a twin sovereign debt and banking crisis. Further negative feedback loops between vulnerable banks, indebted sovereigns and weak economies took hold in several countries and led to acute financial fragmentation along country borders (Hartmann and Smets, 2018). Economic confidence fell, the economy slowed down rapidly and the euro area entered a double-dip recession in the fourth quarter of 2011 until the first quarter of 2013, according to the CEPR business cycle chronology.

Figure 5 shows that the GaR(10%) hovered between 0% and -0.5% during the first half-2011. This is consistent with very mild risks to activity as, up to end-June 2011, the growth rate of GDP for the euro area could have only be expected to run into a slightly negative territory at 10% probability. As of mid-April 2011, the contagion effects of the deterioration in the sovereign CDS spreads started to signal that they may be long-lasting. The situation deteriorated in July 2011. On July 1st, the GaR measure started dropping rapidly, reaching -1.2% in the fourth quarter of 2011 when the euro zone entered into recession. This date precedes the announcement of the Moody's downgrade of Portugal on July 5th. This announcement, along with the continuing fears of a Greek default, could have triggered a sell-off in Spanish and Italian government bonds. By July 18th, the Italian government bond yields had increased by almost 100 basis points, while Spanish bond yields had increased by more than 80 basis points. The downgrading of sovereign ratings escalated and pushed bond rates up to critical levels for peripheral European countries. From April 1st, 2012, the GaR measure returned to its pre-crisis level,

consistently with the first signals of an easing in financial conditions and an exit from the economic recession.

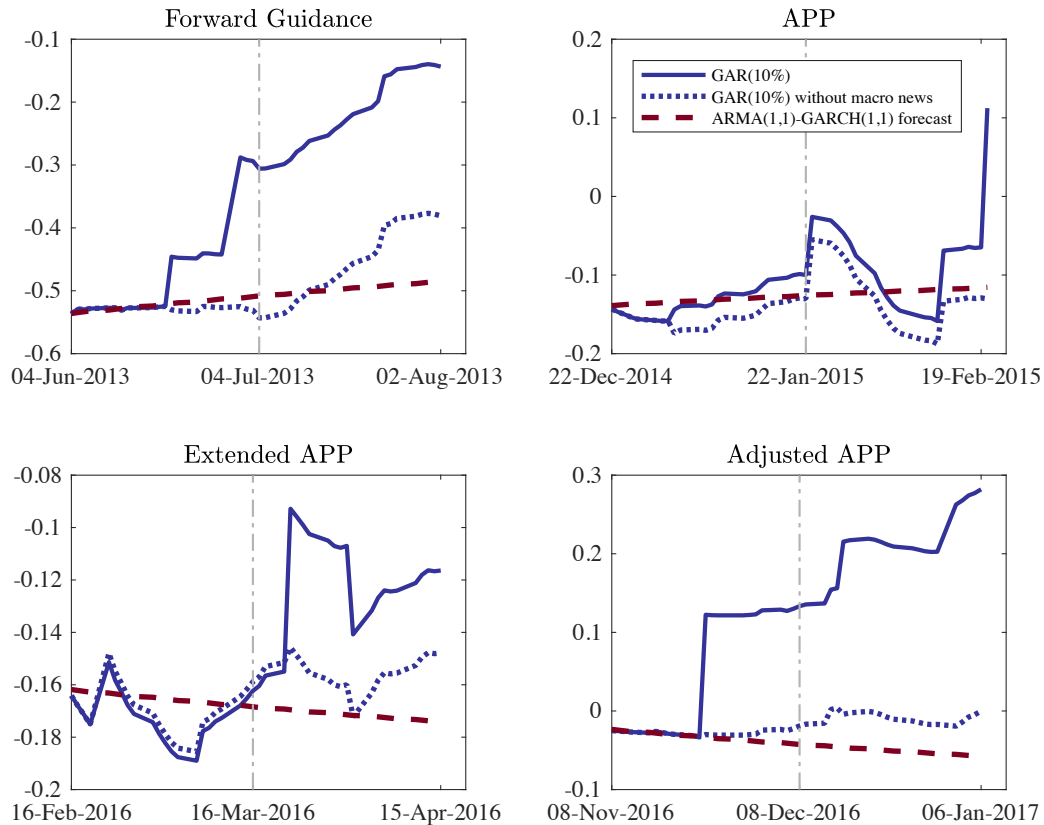
All in all, the results show that our daily GaR(10%) would have been able to correctly track in real-time this specific recession episode. However, and more interestingly, the GaR(10%) measure tends to rapidly fall a quarter ahead of the beginning of the recession, dropping from a value close to zero to about -1% in only a few months. This swift change in the GaR can be interpreted as a possible early signal of recession led by a deterioration in financial conditions.

4.3. Unconventional monetary policy measures announcements. We now turn to the link between the daily GaR measure and the unconventional monetary policy carried out by the ECB. Since 2013, the macroeconomic situation in the euro area has been characterised by increased risks threatening price stability and the anchoring of inflation expectations. Price developments have gradually moved away from values consistent with the ECB definition of price stability, *i.e.* a rate of inflation, as measured by the harmonised index of consumer prices (HICP), close but below 2%. Faced with growing risks of disanchoring expectations, the Eurosystem responded by taking a number of unconventional measures. In particular, four major announcements have been recorded between 2013 and 2018.

First, the ECB has implemented forward guidance about the future course of monetary policy since July 4th, 2013. Forward guidance corresponds to a commitment on the future path of interest rates, so as to influence not only the short-term rates, which reached their lower bound close to zero, but mainly longer-term rates which are to a large extent determined by expectations of future short-term rates. Second, the ECB decided to launch a large asset purchase programme ("*APP*") on January 22nd, 2015. It consists of purchases on the secondary market of private securities and euro-denominated investment-grade securities issued by euro area governments and institutions. The APP programme was subsequently extended and adjusted in several occasions, notably by increasing both duration and total amount of purchases. On March 16th, 2016, the ECB decided to extend the monthly purchases under the APP ("*extended APP*") from 60 billion to 80 billion euros, including a new corporate securities purchase programme (CSPP), starting from April 2016, intended to run until the end of March 2017, or beyond, if necessary. This measure was accompanied by a series of four targeted longer-term refinancing operations (TLTRO II) in order to ease private sector credit conditions and to stimulate credit creation.¹² In addition, the rate on the deposit facility was lowered by 10 basis points to -0.40%. Finally, on December 8th, 2016, the ECB decided to adjust the parameters of the APP ("*adjusted APP*") : (i) the maturity range of the public sector purchase programme broadened by decreasing the minimum remaining maturity for eligible securities from two years to one year and (ii)

¹²The interest rate on these operations, each with a maturity of four years, was fixed at the main refinancing operations rate prevailing at the time of take-up.

FIGURE 6. The GaR 10% and unconventional monetary policy announcements: an event study analysis



Notes: APP: asset purchase programme, Extended APP: extension of the APP, and Adjusted APP: adjusted parameters of the APP. The vertical line corresponds to a specific announcement date. The GaR(10%) corresponds to the lower 10th percentile of the distribution of the expected real GDP growth (plain blue line). The dotted blue line corresponds to the implied GaR(10%) once included dummies with respect to macroeconomic news. The dashed line corresponds to the forecast path of an ARMA(1,1)-GARCH(1,1) representation of the GaR(10%).

purchases of securities under the APP with a yield to maturity below the interest rate on the ECB's deposit facility permitted to the extent necessary. In addition, the APP was announced to be continued at the monthly pace of 80 billion euros until the end of March 2017. From April 2017, the net asset purchases were intended to continue at a monthly pace of 60 billion euros until the end of December 2017, or beyond, if necessary.

In order to analyse the reaction of the daily GaR(10%) to the four monetary policy announcement dates, we perform a quasi event study analysis, in the spirit of [Fama et al. \(1969\)](#). Event studies quantify an event's economic impact in so-called "abnormal returns". In our context, abnormal returns are calculated by deducting the GaR(10%) dynamics that would have been realized if the analyzed event would not have taken place ("normal returns") from the actual dynamics of the GaR(10%). In order

to obtain the equivalent to "normal returns", we estimate an ARMA(1,1)-GARCH(1,1) process for the GAR(10%) over a period starting in 1999 and ending 30 days before a specific event.¹³ We then compute the forecast of the model over a 60 days period, centered on the event. The result of this exercise is provided on Figure 6, in which the four monetary policy announcement dates are represented by the vertical dotted lines. We observe that the daily GaR(10%) (plain blue line) deviates from the forecast path implied by the "normal time" representation during the 60-days event window. That remains the case, even when purged from the effects of macroeconomic news (the announcements of new figures relating to GDP and PMI) through dummy variables (dotted blue line).¹⁴ The GaR(10%) was very reactive to new monetary policy measures by increasing immediately after, sometimes before, each announcement, then exhibiting an upward trend in the following weeks. An exception may be the announcement of the APP, which has been anticipated by the markets for a while. As a result, the impact of the APP announcement on the GAR(10%) may only reflect a fraction of the overall financial market effect of all APP-related news. Consequently, we argue that this new high-frequency GaR measure can be useful for central banks in order to check the immediate effects of their policies on macroeconomic risk and to subsequently adjust adequately their monetary policy stance.

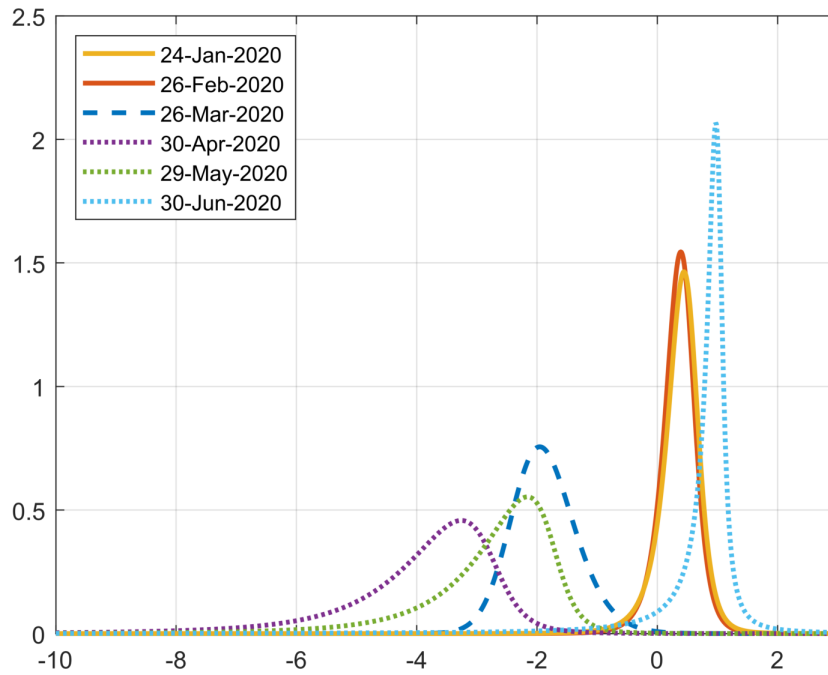
4.4. The Covid-19 pandemic. In this subsection, we focus on the Covid-19 crisis period that affected the euro area, as well as the global economy, during the first half-2020. This shock is the most damaging event since the Great Depression and rather closer to a disaster, in the Robert Barro's sense, than to a classical recession.

During the first two months of 2020, the impact of Covid-19 on the euro area economy has been basically non-significant, as it was not clear that the propagation of the coronavirus coming from China was about to turn into a global pandemic. The first anecdotal evidence came through the disruption of global value chains and diminishing external demand stemming from China. This lack of reaction from financial markets can be seen in Figure 7: there is basically no shift in the conditional distribution of GDP growth for the first quarter of 2020 predicted by our model between January 24th (yellow curve) and February 26th (orange curve). Markets' sentiment started to turn negative in the last days of February, with the Euro Stoxx 50 dropping by about 27% by March 19th. Markets eased only after the ECB announced on March 18th the deployment of a new Pandemic Emergency Purchase Program, with an envelope of 750 billion euros until the end of the year, in complement of an initial smaller plan of 120 billion euros decided on March 12th.

¹³The orders of the ARMA-GARCH process were selected according to standard information criteria (Akaike, Schwarz and Hannan-Quinn).

¹⁴The macroeconomic news concerning new numbers for GDP and PMI are the following: 01/07/2013 (GDP: Eurocoin 2013-Q2), 20/06/2013 (PMI: 6th month), 01/01/2015 (GDP: Eurocoin 2014-Q4), 13/02/2015 (GDP: 2014-Q4), 23/01/2015 (PMI 1st month), 20/02/2015 (PMI: 2nd month), 01/04/2016 (GDP: Eurocoin 2016-Q1), 22/02/2016 (PMI 2nd month), 22/03/2016 (PMI: 3rd month), 02/01/2017 (GDP: Eurocoin 2016-Q4), 23/11/2016 (PMI 11th month), and 15/12/2016 (PMI: 12th month).

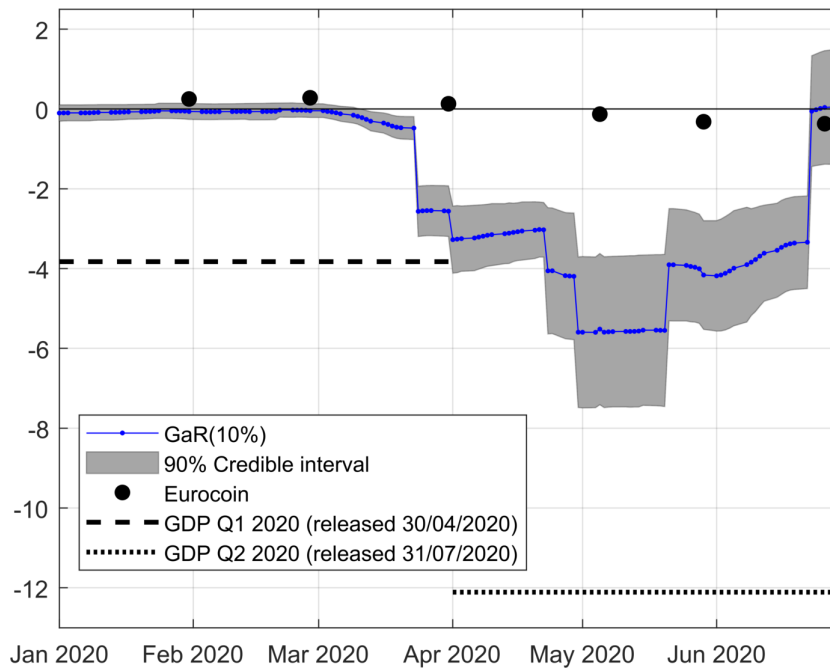
FIGURE 7. Probability density functions of conditional GDP growth



In fact, as shown in Figure 8, the first significant decline in the GaR(10%) coincides with the WHO announcement recognizing the Covid-19 epidemic as a global pandemic, that came on March 11th. Mid-March also corresponds to the start of stringent lockdown measures within euro area countries. Then, we observe a drop at the end of March due to the large fall in stock prices, previously mentioned, and the release of March PMI. This can be also seen in Figure 7, where the predictive distribution of GDP growth for 2020Q1 estimated on March 26th began to sink into negative territory (dashed blue curve). Next, the daily GaR(10%) measure progressively falls to -6% at end of April driven by both PMI and the integration on April 30th of the preliminary estimate of GDP growth for the 2020Q1 into the model. This shift at the end of April is also clearly visible in Figure 7 (dotted purple curve). Starting from May 29th, the GaR(10%) started to increase again, driven by PMI appreciation due to an improvement in business conditions and more optimistic expectations related to a sharp slowdown in the pandemic evolution before the summer 2020.

Two interesting features arise from this empirical analysis. First, we compare our measure with the EuroCoin indicator provided by the CEPR, that can be interpreted as a real-time nowcast of euro area GDP growth. As can be seen on Figure 8, EuroCoin stayed quite high throughout the first half-2020, showing only slightly negative values starting end of April onwards (-0.13), reaching -0.32 in May while the strongly negative GDP growth in 2020Q1 was already known (-3.8% in quarter-on-quarter growth, published on April 30th). As regards 2020Q2, EuroCoin was also unable to reproduce the wide fall in quarterly GDP growth (-12.1%, as published on July 31st), only reaching a minimum

FIGURE 8. The GaR 10% and the Covid-19 pandemic



Note: The GaR(10%) corresponds to the lower 10th percentile of the distribution of the expected real GDP growth.

of -0.64% in August 2020. Although it is fair to say that EuroCoin only aims at tracking a monthly *smoothed* estimate of quarterly GDP growth in the euro area, the deviation from actual GDP growth is however huge. A potential reason underlying this discrepancy is that this index is mainly based on macroeconomic information that comes with a delay and that industrial production information is likely to be over-weighted in the index. In quite contrast, our daily GaR measure has started to provide a clear signal of imminent deterioration of economic activity since mid-March.

Second, despite the timeliness of the signal provided by our daily GaR, its amplitude was fairly lower than the drop observed on GDP growth. This gap can be explained by the nature of the shock underlying the Covid-19 recession. Indeed, it turns out that this recession can be understood as a mix of supply and demand shocks, amplified by an uncertainty shock. On the other hand, the financial shock has been quite limited so far, mainly due to the swift and strong monetary policy response of the ECB. The synchronised reaction of the largest central banks over the world also likely contributed to globally sustain the financial sector. In our view, this explains the limited shift and skewness of the estimated distributions presented in Figure 7. However, the financial risk on GDP growth is still present, as we don't know how the current crisis will evolve in upcoming months. In this respect, we think that our daily GaR measure will continue to be useful to track future risks on economic growth stemming from the financial sector during this major adverse economic event.

5. CONCLUSIONS

This paper extends the quarterly Growth-at-Risk (GaR) approach of [Adrian et al. \(2019\)](#) by accounting for the high-frequency nature of financial conditions. Specifically, we use Bayesian mixed data sampling (MIDAS) quantile regressions to exploit the information content of a financial stress indicator and a financial conditions index to construct real-time high-frequency GaR measures for the euro area. We show that our daily GaR indicator: (i) displays good GDP nowcasting properties, (ii) can provide an early signal of GDP downturns, and (iii) allows day-to-day assessment of the effects of monetary policies. During the first six months of the Covid-19 pandemic period, it has provided a timely indication of tail risks on euro-area GDP. This new high-frequency GaR measure could be efficiently used by monetary policy-makers in order to assess the impact of monetary policy decisions on macroeconomic risk, through the lens of financial market perception.

REFERENCES

- Adams, P., Adrian, T., Boyarchenko, N., Giannone, D., forthcoming. Forecasting Macroeconomic Risks. *International Journal of Forecasting*.
- Adrian, T., Boyarchenko, N., Giannone, D., 2019. Vulnerable growth. *American Economic Review* 109 (4), 1236–1289.
- Andreou, E., Ghysels, E., Kourtellis, A., 2013. Should macroeconomic forecasters use daily financial data and how? *Journal of Business & Economic Statistics* 31 (2), 240–251.
- Azzalini, A., Capitanio, A., 2003. Distributions generated by perturbation of symmetry with emphasis on a multivariate skew t -distribution. *Journal of the Royal Statistical Society: Series B (Statistical Methodology)* 65 (2), 367–389.
- Bernanke, B., Gertler, M., 1989. Agency costs, net worth and business fluctuations. *American Economic Review* 79 (1), 14–31.
- Bernanke, B. S., Gertler, M., Gilchrist, S., 1999. The financial accelerator in a quantitative business cycle framework. In: Taylor, J. B., Woodford, M. (Eds.), *Handbook of Macroeconomics*. Vol. 1. Elsevier, Ch. 21, pp. 1341–1393.
- Carlstrom, C. T., Fuerst, T. S., 1997. Agency costs, net worth, and business fluctuations: A computable general equilibrium analysis. *American Economic Review* 87 (5), 893–910.
- Carriero, A., Clark, T. E., Marcellino, M., 2020. Nowcasting tail risks to economic activity with many indicators. Working Paper 20-13R, Federal Reserve Bank of Cleveland.

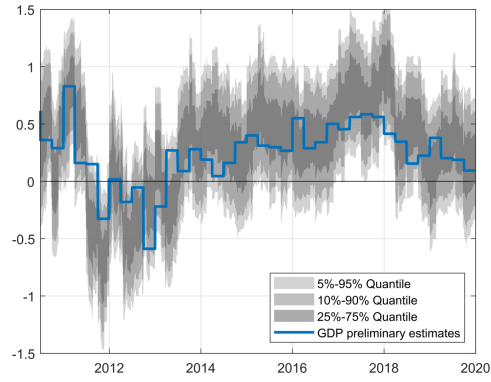
- Christiano, L. J., Motto, R., Rostagno, M., January 2014. Risk Shocks. *American Economic Review* 104 (1), 27–65.
- Claessens, S., Kose, M. A., Terrones, M. E., 2012. How do business and financial cycles interact? *Journal of International Economics* 87 (1), 178–190.
- Clements, M. P., Galvao, A. B., 2009. Forecasting US output growth using leading indicators: an appraisal using MIDAS models. *Journal of Applied Econometrics* 24 (7), 1187–1206.
- De Santis, R. A., Van der Veken, W., 2020. Forecasting macroeconomic risk in real time: Great and covid-19 recessions. Working Paper Series 2436, ECB.
- Diebold, F. X., Mariano, R. S., 1995. Comparing predictive accuracy. *Journal of Business and Economic Statistics* 13 (3), 253–263.
- Fama, E. F., Fisher, L., Jensen, M., Roll, R., 1969. The Adjustment of Stock Prices to New Information. *International Economic Review* 10 (1), 1–21.
- Figueres, J. M., Jarocinski, M., 2020. Vulnerable growth in the euro area: Measuring the financial conditions. *Economics Letters* 191 (C).
- Geweke, J., Amisano, G., 2011. Optimal prediction pools. *Journal of Econometrics* 164 (1), 130–141.
- Ghysels, E., 2016. Macroeconomics and the reality of mixed frequency data. *Journal of Econometrics* 193 (2), 294–314.
- Ghysels, E., Plazzi, A., Valkanov, R., 2016. Why invest in Emerging Markets? the role of conditional return asymmetry. *The Journal of Finance* 71 (5), 2145–2192.
- Giglio, S., Kelly, B., Pruitt, S., 2016. Systemic risk and the macroeconomy: An empirical evaluation. *Journal of Financial Economics* 119 (3), 457–471.
- Gilchrist, S., Zakrajsek, E., June 2012. Credit Spreads and Business Cycle Fluctuations. *American Economic Review* 102 (4), 1692–1720.
- Gneiting, T., Raftery, A., 2007. Strictly proper scoring rules, prediction, and estimation. *Journal of the American Statistical Association* 102 (477), 359–378.
- Gneiting, T., Ranjan, R., 2011. Comparing density forecasts using threshold- and quantile-weighted scoring rules. *Journal of Business & Economic Statistics* 29 (3), 411–422.
- Gonzalez-Rivera, G., Maldonado, J., Ruiz, E., 2019. Growth in stress. *International Journal of Forecasting* 35 (3), 948–966.
- Hall, S. G., Mitchell, J., 2007. Combining density forecasts. *International Journal of Forecasting* 23 (1), 1–13.

- Hartmann, P., Smets, F., 2018. The first twenty years of the European Central Bank: monetary policy. Working Paper Series 2219, European Central Bank.
- Helbling, T., Huidrom, R., Kose, M. A., Otrok, C., April 2011. Do credit shocks matter? A global perspective. *European Economic Review* 55 (3), 340–353.
- Holló, D., Kremer, M., Lo Duca, M., 2012. CISS - a composite indicator of systemic stress in the financial system. Working Paper Series 1426, ECB.
- Hubrich, K., Tetlow, R., 2015. Financial stress and economic dynamics: The transmission of crises. *Journal of Monetary Economics* 70(C), 100–115.
- IMF, Apr. 2019. Global financial stability report.
- Jermann, U., Quadrini, V., February 2012. Macroeconomic Effects of Financial Shocks. *American Economic Review* 102 (1), 238–271.
- Khare, K., Hobert, J. P., 2012. Geometric ergodicity of the Gibbs sampler for Bayesian quantile regression. *Journal of Multivariate Analysis* 112, 108–116.
- Kiyotaki, N., Moore, J., 1997. Credit cycles. *Journal of Political Economy* 105 (2), 211–248.
- Koenker, R., Bassett, G., 1978. Regression quantiles. *Econometrica* 46 (1), 33–50.
- Korobilis, D., 2017. Quantile regression forecasts of inflation under model uncertainty. *International Journal of Forecasting* 33 (1), 11–20.
- Kozumi, H., Kobayashi, G., 2011. Gibbs sampling methods for Bayesian quantile regression. *Journal of Statistical Computation and Simulation* 81 (11), 1565–1578.
- Lima, L. R., Meng, F., Godeiro, L., 2020. Quantile forecasting with mixed-frequency data. *International Journal of Forecasting* 36 (3), 1149–1162.
- Lopez-Salido, D., Stein, J. C., Zakrajsek, E., 2017. Credit-Market Sentiment and the Business Cycle. *The Quarterly Journal of Economics* 132 (3), 1373–1426.
- Mazzi, G.-L., Mitchell, J., 2020. New methods for timely estimates: Nowcasting euro area GDP growth using quantile regression. Statistical working papers, Eurostat.
- Mogliani, M., Simoni, A., 2021. Bayesian MIDAS penalized regressions: Estimation, selection, and prediction. *Journal of Econometrics* 222 (1-C), 833–860.
- Nolan, C., Thoenissen, C., May 2009. Financial shocks and the US business cycle. *Journal of Monetary Economics* 56 (4), 596–604.
- Petronevich, A., Sahuc, J.-G., 2019. A new Banque de France financial conditions index for the Euro Area. *Banque de France Bulletin* 223.

- Pettenuzzo, D., Timmermann, A., Valkanov, R., 2016. A MIDAS approach to modeling first and second moment dynamics. *Journal of Econometrics* 193 (2), 315–334.
- Plagborg-Møller, M., Reichlin, L., Ricco, G., Hasenzagl, T., 2020. When is growth at risk? Tech. rep., *Brooking Papers on Economic Activity*.
- Rodriguez, A., Puggioni, G., April 2010. Mixed frequency models: Bayesian approaches to estimation and prediction. *International Journal of Forecasting* 26 (2), 293–311.
- Rossi, B., Sekhposyan, T., 2019. Alternative tests for correct specification of conditional predictive densities. *Journal of Econometrics* 208 (2), 638–657.
- Schorfheide, F., Song, D., July 2015. Real-Time Forecasting With a Mixed-Frequency VAR. *Journal of Business & Economic Statistics* 33 (3), 366–380.
- Sriram, K., Ramamoorthi, R. V., Ghosh, P., 2013. Posterior consistency of Bayesian quantile regression based on the misspecified Asymmetric Laplace density. *Bayesian Analysis* 8 (2), 1–26.
- Stock, J. H., Watson, M. W., 2004. Combination forecasts of output growth in a seven-country data set. *Journal of Forecasting* 23 (6), 405–430.
- West, K. D., 1996. Asymptotic inference about predictive ability. *Econometrica* 64 (5), 1067–1084.
- Yang, Y., Wang, H. J., He, X., 2016. Posterior inference in Bayesian quantile regression with Asymmetric Laplace likelihood. *International Statistical Review* 84 (3), 327–344.
- Yu, K., Moyeed, R., 2001. Bayesian quantile regression. *Statistics & Probability Letters* 54 (4), 437–447.

APPENDIX A - COMPETING NOWCASTING MODELS

FIGURE A.1. Nowcasting GDP with the combined BMIDAS regressions $y_t = \beta_1 y_{t-1} + \theta'_x \tilde{x}_{i,t-h_d}^{(d)} + \theta'_w \tilde{w}_{t-h_m}^{(m)} + \epsilon_t$



Note: $\tilde{x}_{i,t}^{(d)}$ denotes either the FCI ($i = 1$) or the CISS ($i = 2$). Predictive densities are combined using the QWPS metrics for the computation of combination weights.

FIGURE A.2. Nowcasting GDP with the BQAR(1) regression $y_t = \beta_1(\tau)y_{t-1} + \zeta_1 \tilde{v}_t + \zeta_2 \sqrt{\sigma \tilde{v}_t} \omega_t$

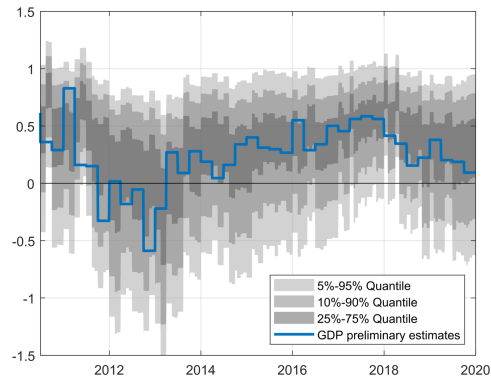


FIGURE A.3. Nowcasting GDP with the BAR(1) regression $y_t = \beta_1 y_{t-1} + \epsilon_t$

